The electrochemical corrosion behaviour of Ti-48Al-2Nb-0.7Cr-0.3Si alloy in 3.5%NaCl

Steven Magogodi[1,2*], *Maria* Mathabathe[1], *Amogelang* Bolokang[1,3], and *Charles* Siyasiya[2]

[1]Council of Scientific Industrial Research, Materials Science and Manufacturing, Light metals, Meiring Naude Road, P O Box 395 Pretoria, South Africa.
[2]Department of Material Science and Metallurgical Engineering, Faculty of Engineering, Built Environment and Information Technology, University of Pretoria, South Africa.
[3]Department of Physics, University of the Western Cape, Private Bag X 17, Bellville 7535, South Africa

Abstract. Titanium aluminides (TiAl) have attracted industrial interest, particularly for high temperature applications owing to their promising mechanical properties. Due to the application of these materials to the marine environment it is therefore important to understand their performance under such conditions. In this study, the corrosion behaviour of Ti-48Al-2Nb-0.7Cr-0.3Si alloy produced by vacuum arc melting was investigated using the potentiodynamic polarization method. The corroded surface and Ti-Al phases were investigated by scanning electron microscopy (SEM), optical microscopy, and X-ray diffraction (XRD). Hardness was examined by a Vickers micro hardness tester with a diamond indenter. Pitting was observed to occur within the surface defects and caused severe corrosion.

1 Introduction

The world is facing high demand for energy provision and that is leading to the search for high-performance materials that are lightweight, have high strength, and exhibit excellent corrosion resistance in marine and corrosive atmospheres [1, 2]. The TiAl alloys are promising high-performance materials owing to their low density, high specific strength, good corrosion resistance, and reasonable high-temperature mechanical properties [3, 4]. These materials are ideal for replacing nickel-based super-alloys in low-pressure turbine blades within the aerospace industry due to their low density and high strength [5]. Furthermore, TiAl-based alloys exhibit excellent corrosion resistance when compared to titanium alloys such as Ti6Al4V and that is attributed to high aluminium (Al) content within the alloy matrix [6]. The Al has the capability of forming a surface protective alumina layer (Al_2O_3) which is responsible for shielding the materials from further corrosion [7].

The major application of military aircraft in the marine environment exposes TiAl turbine blades within the aero-engine components to NaCl which may get accumulated on their surface. Within the marine environment, these materials must be able to withstand harsh

* Corresponding author: magogodistevens@gmail.com

corrosive environments that might be experienced due to volatile chloride ions (Cl^-). These volatile Cl^- have the capability to react with Ti and Al and thus degrade the surface protective scale of the TiAl-based alloys and consequently leading to premature failure [8, 9].

Even though TiAl-based alloys retain interesting mechanical properties, they suffer from poor ductility and fracture toughness at room temperature [8, 9]. Such room temperature ductility limits the fabrication of these alloys [6]. The addition of the alloying elements such as Nb, Cr, and Si, to TiAl-based alloys, is known to improve their low-temperature ductility, solute solution strengthening, and oxidation resistance [10-13]. Furthermore, fabrication of the TiAl-based alloys can be achieved through the process of powder metallurgy, ingot metallurgy, investment casting, additive manufacturing, selective laser melting, and vacuum arc re-melting (VAR) [14 -17]. Ingot metallurgy and investment casting retain the issue of high production costs and create challenges such as coarse grains, microstructure segregation, solidification shrinkage, and room temperature ductility [14, 19]. Powder metallurgy is a promising cost-effective fabrication technique that can achieve near net shape and it also aids control over factors such as alloying composition and microstructure homogeneity and refinement [18]. VAR is a re-melting technique that is frequently used in the fabrication of high-performance materials such as the fabrication of special steel, nickel-base alloys, and reactive metals such as titanium and zirconium [17]. Materials such as titanium and its alloys have a high affinity for oxygen which is considered contamination during melting or heat treatment [20]. Therefore, redox reaction is highly limited in VAR to ensure insignificant deformability.

The TiAl alloys composed of α_2/γ-TiAl duplex microstructure are known to exhibit enhanced ductility and good room temperature strength than those of γ-TiAl single phase [20]. The microstructure of the TiAl alloys can be controlled to obtain a duplex microstructure depending on the chemical composition and heat treatment [21]. The aim of this work was to fabricate the Ti-48Al-2Nb-0.7Cr-.03Si (at. %) alloy consisting of ($\alpha_2+\gamma$) dual phases through the powder metallurgy route, and cast it through VAR, then study its electrochemical behaviour in marine atmosphere.

2 Material and methods

2.1 Material

The Ti-48Al-2Nb-0.7Cr-0.3Si (at. %) alloy was fabricated through the powder metallurgy route. Pure elemental powders of (a) Ti, (b) Al, (c) Nb, (d) Cr, and (e) Si as shown in Fig. 1, were blended in a Turbula shaker mixer and then cold pressed using Enerpac hydraulic press with a die of 51mm diameter. The different elemental morphologies, sizes, and shapes of the metallic powders are presented in Table 1. The green compact was subjected to vacuum arc melting and it was melted three times to promote homogeneity within the microstructure, and the arc melted button with the dimensions of 38 × 38 × 13 mm^3 is shown in Fig.1 (f).

Table 1: Particle size and morphology of the elemental powders

Elements	Ti	Al	Nb	Cr	Si
Morphology	Angular	Spherical	Angular	Angular	Angular
Particle size(μm)	30.51	74.0	23.89	126.0	8.90

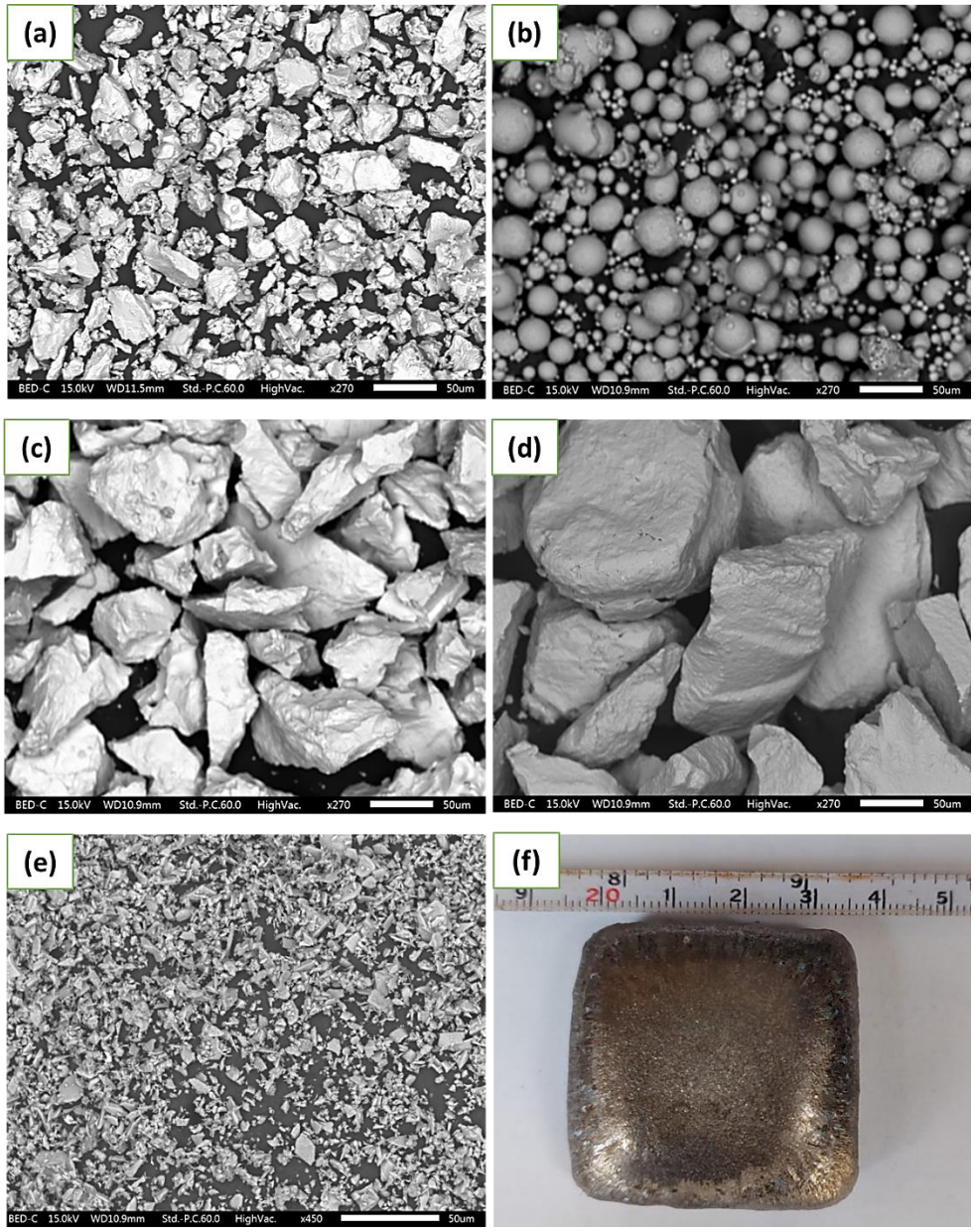

Fig. 1. SEM micrographs of the; (a) Ti; (b) Al; (c) Nb; (d) Cr; (e) Si powder particles and; (f) VAR melted button.

2.2 Heat reatment

The VAR melted Ti-48Al-2Nb-0.7Cr-0.3Si (at. %) alloy was heat treated at 1250 ºC for 1h using a tube furnace under argon-rich atmosphere. The furnace temperature was ramped at 20 ºC/min from room temperature up to 1250 ºC and held there for one hour before cooling down to room temperature within the furnace.

2.3 Sample preparation and characterization

The specimen for electrochemical dissolution was machined into a 2 cm diameter and 6 mm thickness while the as-cast was machined 10 × 10 × 2 mm^3 through wire-electrical discharge machining. The metallographic preparation was performed on as-cast, heat-treated and corrosion samples. All samples were ground up to 4000 SiC grit paper to a mirror-like finish. The Kroll reagent was applied to the samples by immersing them in the etchant in order to reveal their microstructures. Optical microscopy and SEM were used for surface morphology and microstructural investigations. The phase analysis of the TiAlNbCrSi was characterized by XRD with Cu Kα radiation λ=1.54Å and the samples were scanned within a 2θ range of 20º to 100º.

2.4 Micro hardness test

The micro hardness property of the fabricated TiAlNbCrSi alloy was performed using the FUTURE-TECH FM-700 micro-hardness tester. The load of 500 gf ($HV_{0.5}$) was applied on the surface of the sample for indention with a dwell time of 10 seconds and the diagonal indent was separated by a spacing of 500 μm for ten points and the average was recorded.

2.5 Corrosion test

The electrochemical behaviour of the Ti-48Al-2Nb-0.7Cr-0.3Si (at. %) alloy was investigated in a 3.5% NaCl solution using autolab-potentionstat for defining its linear polarisation. The three-electrode cell system comprising of Ag/AgCl as a reference electrode (RE), platinum wire as a counter electrode (CE), and TiAl sample as a working electrode (WE). The 1 cm^2 surface area of the WE was exposed to the electrolyte. In order to obtain the polarization curves, two tests were performed in order to study the electrochemical behaviour of the alloy immersed in 3.5 % NaCl electrolyte. For the first test, the potential was scanned in a forward direction from -1.9 V to 1.1 V against RE at a scan rate of 0.001 V/s. In the second test, the sample was ground through the metallographic process to remove the surface protective oxide and the potential was scanned in a forward direction from -1.9 to 1.1 V against RE at a scan rate of 0.001 mV/s as per [6].

3 Results and discussion

3.1 Microstructure and phase analysis

Fig. 2 shows the micrographs of the (a) as cast and (b) heat treated samples. The micrographs illustrate the lamellar structure comprising (α_2+γ)-TiAl dual-phases. The alpha (α_2) phases are shown by dark grey while the gamma (γ) phases are shown by light grey [22]. The as-cast sample show some pores on the surface. The heat-treated sample is observed to have a growth in a lamellar structure consisting of colonies of alternating (α_2+γ) phases [22, 23] when compared to as cast sample and growth in lamellar structure as the sample is homogenized at 1250 ºC for 1 h. There are still some minimal micro-pores observed in a heat treated sample.

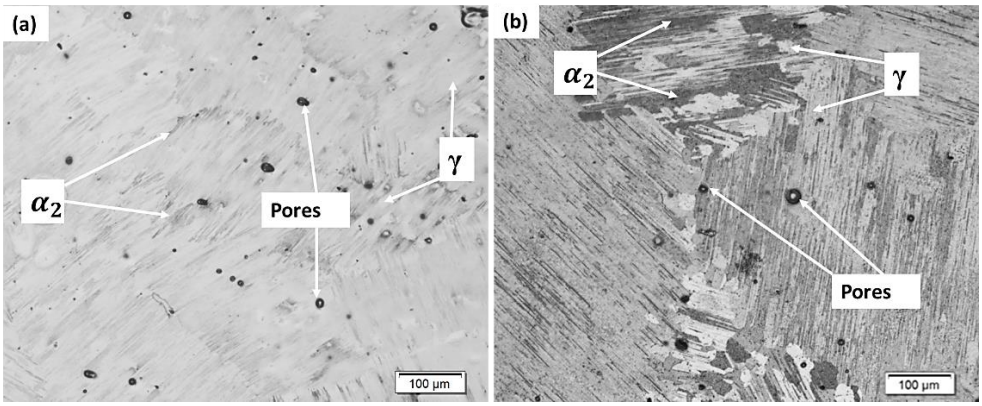

Fig. 2. Optical micrographs of the Ti-48Al-2Nb-0.7Cr-0.3Si (at. %) alloy (a) as cast and (b) heat treated.

Fig.3 shows the XRD pattern of the as cast and heat treated samples in 2θ range of 20 - 100. The pattern shows the peaks corresponding to the micrographs in Fig. 2 which displays the crystal structures of the hexagonal close-packed α_2-Ti_3Al and face-centered tetragonal γ-TiAl phases. According to the Ti-Al phase diagram [21], various microstructures can be produced depending on the presence of Al content and heat treatment temperature. Heat treatment was used to homogenize the ($\alpha_2 + \gamma$)-TiAl dual phase and the attaining of such phases is confirmed by XRD. The XRD pattern of the as cast show the γ-TiAl as a major phase as shown by high with high intensity at 2θ of 45.4 and this peak is observed to decrease in intensity after heat treatment. The intensity decrease on heat treated sample means that the unstable alpha phases dissolved for the formation of stable phases [6].

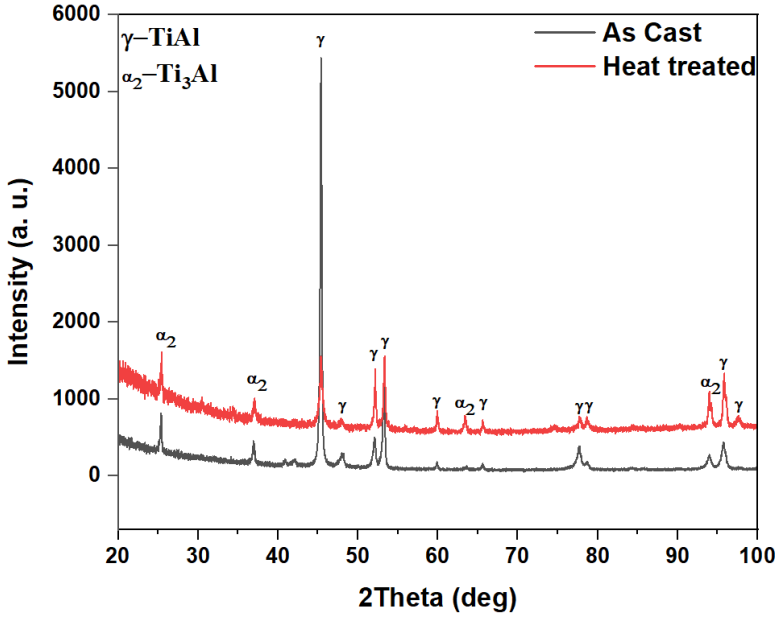

Fig. 3. X-ray diffraction pattern of the heat treated Ti-48Al-2Nb-0.7Cr-0.3Si alloy (at.%).

3.2 Micro hardness analysis

The micro hardness was performed in as-cast and heat-treated samples. Fig. 4 presents the as-cast sample which was recorded to have a hardness of 361.69 $HV_{0.5}$, whereas the heat-treated sample was having a hardness of 289.26 $HV_{0.5}$. Heat treatment is encouraging boundary growth and relieves the internal stress that is caused by the high density of internal boundaries after melting [24] consequently leading to a slight decrease in the micro hardness. It is worth noting that the sample in Fig. 2 (b) has resulted in larger grain after heat treatment as evidence of grain growth and internal stress relief.

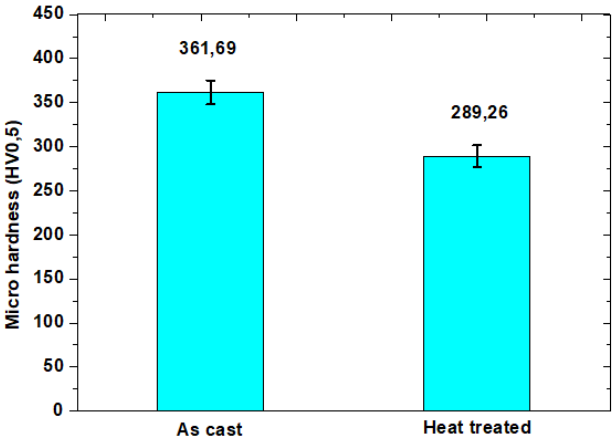

Fig. 4. Micro hardness properties of the as cast and heat treated Ti-48Al-2Nb-0.7Cr-0.3Si (at. %) alloy.

3.3 Corrosion analysis

The effect of the 3.5 % NaCl solution was investigated on the electrochemical dissolution behaviour through the potentiodynamic polarization curve. The 3.5% NaCl is known to simulate the marine environment [25] and it has been observed to have some effect on the surface of the TiAl-based alloys [6, 25, 26]. Table 2 displays the extrapolated Tafel electrochemical parameters of the Ti-48Al-2Nb-0.7Cr-0.3Si (at. %) alloy in 3.5% NaCl at room temperature. The linear polarisation curve of the investigated Ti-48Al-2Nb-0.7Cr-0.3Si (at. %) alloy is presented in Fig. 5, and the corroded microstructure is presented in Fig 6.

Table 2. Corrosion parameters for TiAl alloys under 3.5% NaCl electrolyte.

$\mathbf{E_{corr}}$(V)	$\mathbf{I_{corr}(A/cm^2)}$	$\mathbf{E_{pit}(V)}$	Passivation (V)	Corrosion rate (mm/year)
-0.6283	3.196E-06	0.3413	0.9696	0.64570

The polarization curve shows a negative corrosion potential (E_{corr}) of -0.6283 V, corrosion current density (I_{corr}) of 3.196 x 10^{-6} A/cm^2 and a corrosion rate of 0.64570 mm/year. The current density of the anodic curve shows stable behaviour before reaching the pitting potential (E_{pit}) of 0.3413 V, thereafter it increases sharply. The current density increment goes with local corrosion on the pores of the alloy, so the alloy stayed in an equilibrium state from the corrosion potential up to the pitting potential where pitting corrosion occurred at a rapid rate with the current density increase. The alloy presents stable passivation appearances

with the interval of about 0.9696 V. The stable passivation characteristics is attributed to the formation of a passive film of Al_2O_3/TiO_2 on the surface during anodic corrosion. While the pitting potential is attributed to the aggressive chloride ions penetrating the passive layer from the pores and easily breaking the protective film exposing the Ti-Al matrix to the electrolyte. Consequently, leading to the current density increase.

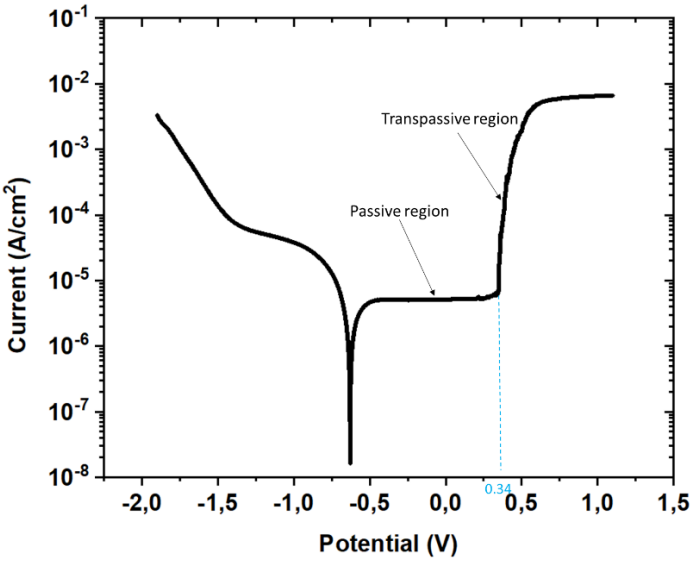

Fig. 5. Potentiodynamic polarization curves of the Ti-48Al-2Nb-0.7Cr-0.3Si (at. %) alloy in 3.5%NaCl electrolyte.

Fig. 6 (a) presents the corroded morphology of the sample after the electrochemical polarization in 3.5% NaCl solution. A large pit is observed to occur on the surface of the alloy which is in agreement with the polarisation curve from Fig. 5. The higher magnification is presented in Fig. 6 (b) which reveals the lamellar colonies where the corrosion medium was attacking and exposing the Ti-Al matrix due to the aggressive chloride ions. Moreover, few pits existed on the surface of the corroded sample which is in agreement with the behaviour of the anodic curve.

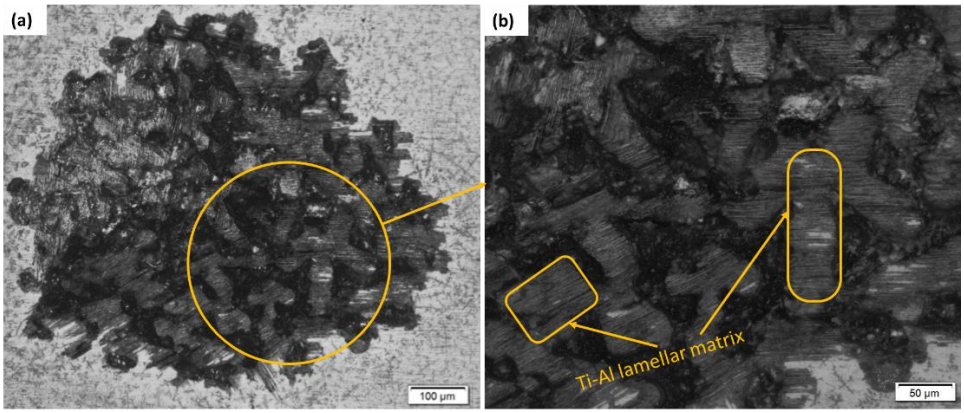

Fig. 6. (a) The optical micrographs of the Ti-48Al-2Nb-0.7Cr-0.3Si (at.%) alloy after chemical polarisation in 3.5%NaCl electrolyte and (b) the magnifications.

4 conclusion

The TiAl alloys are lightweight materials that are regarded as promising candidates for low-pressure turbine blades within the aero-engines. This study was aiming to fabricate the Ti-48Al-2Nb-0.7Cr-0.3Si (at. %) alloy containing (α_2 +γ)-dual phase and examine the alloy behaviour under electrochemical dissolution in 3.5% NaCl. SEM, optical microscope, and XRD were used to study the microstructure and phases of the sample and the following conclusion is made.

- The Ti-48Al-2Nb-0.7Cr-0.3Si (at. %) alloy with (α_2 +γ)-dual phase was successfully fabricated.
- The alloy displays a fully lamellar structure with altering colonies of α_2-Ti_3Al and γ-TiAl dual phases.
- Heat treatment has reduced the micro-hardness of the alloy due to grain growth and relieved internal stress.
- The potentiodynamic polarization curve exhibited stable passive current density as a result of Al_2O_3/TiO_2, pitting is observed due to surface pores, and the alloy show good corrosion resistance as it exhibited a low corrosion rate. However, the surface pores make it easier for volatile Cl^- ions to attack the Ti-Al matrix and lead to pitting.

5 References

1. J. Pang, D.J. Blackwood. *Corrosion of titanium alloys in high temperature near anaerobic seawater*. Corrosion Science, **105**, 17-24 (2016).
2. I.V. Gorynin. *Titanium alloys for marine application. Materials Science and Engineering*: A, **263(2)**, 112-116 (1999.).
3. L.K. Wu, W.Y. Wu, J.L. Song, G.Y. Hou, H.Z. Cao, Y.P. Tang, G.Q. Zheng. *Enhanced high temperature oxidation resistance for γ-TiAl alloy with electrodeposited SiO2 film*. Corrosion Science, **140**, 388-401 (2018).
4. Y. Garip, O. Ozdemir. *Comparative study of the oxidation and hot corrosion behaviors of TiAl-Cr intermetallic alloy produced by electric current activated sintering*. Journal of Alloys and Compounds, **780**, 364-377 (2019).
5. W.X. Hua. *Review of Alloy and Process Development of Ti-Al Alloys [J]*. Intermetallics, **14(1)**, 114-1 (2006).
6. L.R. Kanyane, A.P. Popoola,S. Pityana, M. Tlotleng. *Heat-treatment effect on anti-corrosion behaviour and tribological properties of LENS in-situ synthesized titanium aluminide*. International Journal of Lightweight Materials and Manufacture, **5(2)**, 153-161 (2022).
7. Z. Tang, F. Wang, W. Wu. *Effect of a sputtered TiAlCr coating on hot corrosion resistance of gamma-TiAl*. Intermetallics, **7(11)**, 1271-1274 (1999).
8. M. Mitoraj-Królikowska, E. Godlewska. *Hot corrosion behaviour of (γ+ α2)-Ti-46Al-8Nb (at.%) and α-Ti-6Al-1Mn (at.%) alloys*. Corrosion Science, **115**,18-29 (2017).
9. Z. Tang, F. Wang, W. Wu. *Hot-corrosion behavior of TiAl-base intermetallics in molten salts*. Oxidation of Metals, **51(3)**, 235-250 (1999).
10. N.A. Nochovnaya, P.V. Panin, A.S. Kochetkov, K.A. Bokov. *Modern refractory alloys based on titanium gamma-aluminide: Prospects of development and application*. Metal Science and Heat Treatment, **56(7)**, 364-367 (2014).

11. H. Clemens, A. Bartels, S. Bystrzanowski, H. Chladil, H. Leitner, G. Dehm, R.Gerling, F.P. Schimansky. *Grain refinement in γ-TiAl-based alloys by solid state phase transformations*. Intermetallics, **14(12)**, 1380-1385 (2006).
12. H. Saage, A.J. Huang, D. Hu, M.H. Loretto, X. Wu. *Microstructures and tensile properties of massively transformed and aged Ti46Al8Nb and Ti46Al8Ta alloys*. Intermetallics, **17(1-2)**, 32-38 (2009).
13. D. Hu, A.J. Huang, X. Wu, X. *On the massive phase transformation regime in TiAl alloys*: The alloying effect on massive/lamellar competition. Intermetallics, **15(3)**, 327-332 (2007).
14. M. Bünck, T. Stoyanov, J. Schievenbusch, H. Michels, A. Gußfeld. *Titanium aluminide casting technology development*. JOM, **69(12)**, 2565-2570 (2017).
15. J. Campbell. Complete casting handbook: metal casting processes, metallurgy, techniques and design. Butterworth-Heinemann, 2015.
16. K. Kothari, R. Radhakrishnan, N.M. Wereley, T.S. Sudarshan. *Microstructure and mechanical properties of consolidated gamma titanium aluminides*. Powder metallurgy, **50(1)**, 21-27 (2007).
17. N.M. Mathabathe, A.S. Bolokang, G. Govender, C.W. Siyasiya, R.J. Mostert. *Cold-pressing and vacuum arc melting of γ-TiAl-based alloys*. Advanced Powder Technology, **30(12)**, 2925-2939 (2019).
18. Z.Z. Fang, J.D. Paramore, P. Sun, K.R. Chandran, Y. Zhang, Y. Xia, F. Cao, M. Koopman, M. Free. *Powder metallurgy of titanium–past, present, and future.* International Materials Reviews, **63(7)**, 407-459 (2018).
19. S. Fager Franzén, J. Karlsson. Titanium Aluminide Manufactured by Electron Beam Melting (Master's thesis), 2010.
20. X.J. Jiang, Y.Y. Zhang, N. Yang, S.Q Wang, Q.X. Ran. *The effect of 0.3 wt% oxygen on mechanical properties of a TiZrAl alloy prepared by vacuum arc melting*. Vacuum, **175**, 109248 (2020).
21. Y. Mishin, C. Herzig. *Diffusion in the Ti–Al system*. Acta materialia, **48(3)**, 589-623 (2000).
22. H. Clemens, S. Mayer. *Design, processing, microstructure, properties, and applications of advanced intermetallic TiAl alloys*. Advanced engineering materials,**15(4)**, 191-215 (2013).
23. H. Clemens, A. Bartels, S. Bystrzanowski, H. Chladil, H. Leitner, G. Dehm, R. Gerling, and F.P. Schimansky. *Grain refinement in γ-TiAl-based alloys by solid state phase transformations*. Intermetallics, **14(12)**, 1380-1385 (2006).
24. A. Shabani, M.R. Toroghinejad, A. Shafyei, R.E. Logé. *Evaluation of the mechanical properties of the heat treated FeCrCuMnNi high entropy alloy*. Materials Chemistry and Physics, **221**, 68-77 (2019).
25. A.H. Seikh, A. Mohammad, E.S.M. Sherif, A. Al-Ahmari. *Corrosion behavior in 3.5% NaCl solutions of γ-TiAl processed by electron beam melting process*. Metals, **5(4)**, 2289-2302 (2015).
26. Y. Wang, Z. Xu, A. Zhang. *Electrochemical dissolution behavior of Ti-45Al-2Mn-2Nb+ 0.8 vol% TiB2 XD alloy in NaCl and $NaNO_3$ solutions*. Corrosion Science, **157**, 357-369 (2019).